

Received November 7, 2021, accepted December 6, 2021, date of publication December 13, 2021, date of current version December 21, 2021.

Digital Object Identifier 10.1109/ACCESS.2021.3134990

Advance the Efficiency of an Active Suspension System by the Sliding Mode Control Algorithm With Five State Variables

TUAN ANH NGUYEN 

Department of Automotive Engineering, Thuyloi University (TLU), Dong Da, Hanoi 100000, Vietnam

e-mail: anhngtu@tlu.edu.vn

ABSTRACT Roughness on the road is the main cause of the oscillation when the vehicle travels. The suspension system plays a role in maintaining the stability of the vehicle in fluctuating states. To improve comfort and smoothness, the active suspension system is used to replace the conventional passive suspension system. The performance of the active suspension system depends on the pre-designed controller. Linear control algorithms cannot guarantee oscillation requirements in all cases. Therefore, the use of a nonlinear control method is necessary. In this paper, the SMC (Sliding Mode Control) algorithm is proposed to control the operation of the active suspension system. To optimize this algorithm, five state variables were considered. Besides, the output signal of the model has been considered by the fifth derivative, and the error signal is also considered the fourth derivative. This is a completely novel and unique method. The simulation is done in the MATLAB-Simulink environment. According to this result, the displacement and acceleration of the sprung mass was significantly reduced when the vehicle used the active suspension system controlled by the SMC algorithm. These values only reach 14.4% and 14.1% compared to the case of the vehicle using the mechanical suspension system. The effect of the SMC algorithm is extremely positive. This will be the basis for developing more complex control algorithms in the future.


INDEX TERMS Vehicle dynamics, sliding mode control, hydraulic actuator, nonlinear controller, active suspension system.

I. INTRODUCTION

Vehicle oscillations can affect the smoothness and comfort of traveling on the road. There are many causes of oscillation, among which roughness on the road is the main cause. In studies about oscillations, several types of pavement roughness are commonly used, such as cyclic (sine wave), step, and random. The random stimulus is frequently the most realistic description. The oscillations of the vehicle can be assessed through the oscillations of the sprung mass. Typically, data on displacement, acceleration, roll angle, and angular acceleration are of greater interest [1], [2]. The average and maximum values of these parameters are considered during the calculation [3].

The suspension system on the vehicle helps to regulate and extinguish the oscillations. For a conventional passive suspension system, the stiffness of the springs and dampers is unchanged. Therefore, the smoothness of the vehicle

will not be guaranteed. To improve this situation, air suspension has been used on some high-end cars. According to Eskandary *et al.*, the stiffness of the air spring can vary based on the pressure of the system [4]. In studies of air suspension systems, the GENSYS model is often used [5]. Besides, the damper stiffness can also be changed thanks to the semi-active suspension system [6]. This system uses an electronic damper which is controlled via a previously set controller. When current is applied to the damper, a magnetic field will appear inside. As a result, the metal particles will be more tightly arranged. This leads to an increase in the stiffness of the damper [7]. However, the effectiveness of the semi-active suspension system is still not guaranteed in some complex cases. According to Jiregna and Sirata, the active suspension can improve the ride comfort more optimally [8]. The active suspension system is equipped with a hydraulic actuator at each suspension system position. This is a hydraulic cylinder, and it is shown in Figure 2. The hydraulic pressure inside the cylinder depends on the displacement of the servo valves. According to [9], these

The associate editor coordinating the review of this manuscript and approving it for publication was Zheng Chen .

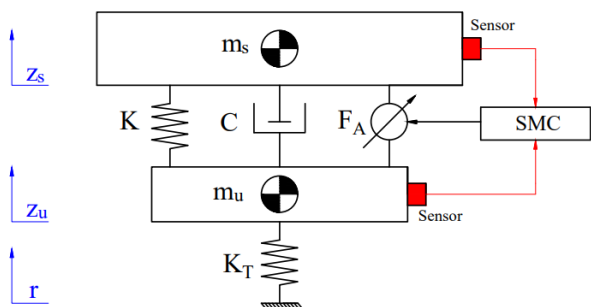


FIGURE 1. Quarter dynamics model.

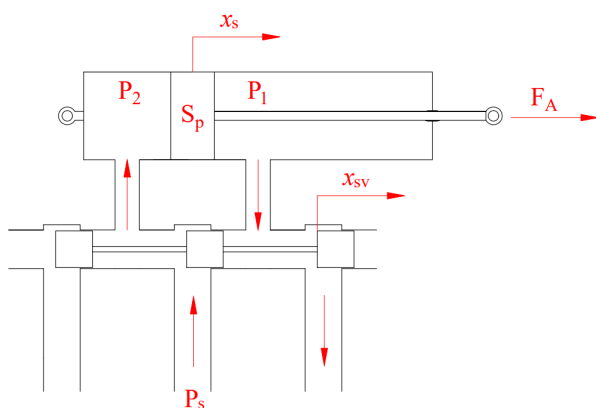


FIGURE 2. Hydraulic actuator.

valves are controlled based on the current signal provided by the controller. At that time, an impact force will be generated, and it acts on the sprung mass and the unsprung mass in opposite directions. The performance of the system will depend entirely on the control algorithm of the controller.

There are many methods used to control the active suspension system. Among them, linear control methods are commonly used. Anh introduced the PID algorithm for the quarter dynamics model in [10]. According to Anh, this controller has a low cost and high durability. The PID controller consists of three stages: proportional stage, integral stage, and derivative stage. For each stage, a corresponding coefficient is needed. If the integral stage of the system is ideal, i.e., $K_I = 0$, the controller is called PI [11]. The controller parameters can be selected by an experimental process. Besides, Genetic Algorithms (GA) can also be used to optimize these parameters. This was done by Metered *et al.* in their study [12]. To improve the efficiency of the PID controller, the ANN algorithm is integrated into the system [13]. Besides, equipping two hydraulic actuators which control two objects separately also provides higher stability than other cases. This was pointed out in Nguyen’s article [14]. However, the PID algorithm only applies to the SISO system. Therefore, if the object has many inputs and many outputs, it is necessary to choose an algorithm suitable for the MIMO system. According to Nagarkar *et al.*, the LQR algorithm is suitable for this purpose [15]. The LQR control algorithm minimizes the cost function based on

the state matrices of the system. In some cases, the signal of the system is still unstable. Therefore, a Gaussian filter is integrated for the controller. This idea was introduced by Chai and Sun. It is called the LQG controller [16]. This algorithm provides higher stability with noise signals removed [17]–[20]. Besides, the active suspension control model using the LPV algorithm was also performed by Rodriguez-Guevara *et al.* According to them, this algorithm uses continuously changing parameters to fit the selected model [21].

The linear control method can only meet the requirements of the vehicle’s stability under certain conditions. To ensure the best oscillation efficiency, nonlinear control and intelligent control methods need to be used. In [22], Zhao *et al.* used an adaptive control algorithm for the saturation actuator. According to Huang *et al.*, vehicle oscillations will change continuously to respond well to external stimuli [23]. This is the essence of the adaptive control method that was used in their study. If the adaptive algorithm is properly optimized, the response will be a smooth function. As a result, the vehicle’s smoothness is significantly improved. This was demonstrated in the paper of Fu *et al.* [24]. For this method, the signals can be obtained from the sensor or from the camera which is integrated into the vehicle body [25]. Besides, the robust control algorithm also helps to reduce vehicle oscillation in many situations [26]. In [27], Wang *et al.* performed a simulation of vehicle oscillations using the active suspension system, which is controlled by a robust algorithm in the case of steering. Accordingly, the value of the roll angle has been greatly reduced when the robust controller is used. In addition, the intelligent control method using the Fuzzy algorithm also brings a stable effect to the system [28]. According to Soleymani *et al.*, the input data of the controller will undergo a fuzzification process. Based on the pre-established fuzzy rule, the defuzzification process is performed to find the output value [29]. The Fuzzy controller can use one or more input parameters to serve the control process. Its efficiency is also quite high [30]–[32]. Furthermore, ANN-based algorithms improve control process stability in a variety of situations [33], [34].

The SMC control algorithm has also been applied to the active suspension system. In [35], Nguyen used the SMC controller for the quarter dynamics model. However, the hydraulic actuator of the system is not considered. In [36], the hydraulic actuator is represented only through a single linear equation. Although Bai and Guo used five state variables. However, the system’s error is only derivative for the third time. Therefore, the efficiency of the controller is still not guaranteed. When the SMC algorithm was combined with other algorithms, the controller efficiency was enhanced [37]–[40].

This research aims to establish a novel SMC algorithm for the active suspension system model. In this paper, the SMC algorithm uses five state variables, corresponding to the quarter dynamics model and the dynamics model of the

hydraulic actuator. Unlike in other papers, the output signal of the system in this research is considered by the fifth derivative. Besides, the error of the system is also considered for the fourth derivative. This is a novel solution that is highly effective. The content of the paper consists of four sections. In the first section, oscillations and suspension system problems are introduced. In addition, the literature review process is carried out in this section. In the second section, the vehicle's oscillation model and control algorithm design process are conducted. The results of the simulation process are given in the third section. The simulation is conducted in the MATLAB-Simulink environment with specific conditions. In the last section, some conclusions and future recommendations are indicated. The content of the paper is presented below.

II. MATERIAL AND METHOD

A. QUARTER DYNAMICS MODEL

To simulate the vehicle's oscillations, a quarter dynamic model is considered (Figure 1).

The equations describing the vertical oscillations of the sprung mass and unsprung mass are given as follows:

$$m_s \ddot{z}_s = K(z_u - z_s) + C(\dot{z}_u - \dot{z}_s) + F_A \tag{1}$$

$$m_u \ddot{z}_u = K_T(r - z_u) - K(z_u - z_s) - C(\dot{z}_u - \dot{z}_s) - F_A \tag{2}$$

The impact force F_A is generated by the hydraulic actuator. When current is supplied from the controller to the actuator, the servo valve moves. The dependence between the displacement of the servo valve x_{sv} and the control current $i(t)$ is shown in equation (3):

$$x_{sv} = \frac{1}{\tau} \int (k_{sv} i(t) - x_{sv}) dt \tag{3}$$

As the valves move, the pressure of the two chambers inside the cylinder changes. The change in pressure is a complex multivariable function. According to [14]:

$$\Delta P = \sigma_3 \int (x_{sv} \sqrt{P_s - \text{sgn}(x_{sv}) \Delta P}) dt - \sigma_2 \int \Delta P dt - \sigma_1 S_p \int \dot{x}_s dt \tag{4}$$

The impact force F_A is proportional to the change in pressure. Therefore:

$$F_A = S_p \Delta P = S_p \left(\begin{matrix} \sigma_3 \int x_{sv} \sqrt{P_s - \text{sgn}(x_{sv}) \Delta P} dt \\ -\sigma_2 \int \Delta P dt - \sigma_1 S_p \int \dot{x}_s dt \end{matrix} \right) \tag{5}$$

Because: $\begin{cases} |k_{sv}| \approx |\tau| \\ |\dot{x}_{sv}| \ll \tau \end{cases}$

From (3):

$$\Rightarrow x_{sv} \approx k_{sv} i(t) \tag{6}$$

Because: $\text{sgn}(x_{sv}) \Delta P \ll P_s$

Taking the derivative of both sides of (5), the equation for determining the impact force is linearized as follows:

$$\dot{F}_A = \rho_1 i(t) - \rho_2 F_A - \rho_3 (\dot{z}_s - \dot{z}_u) \tag{7}$$

where:

$$\rho_1 = S_p \sigma_3 \sqrt{P_s} k_{sv} \quad \rho_2 = \sigma_2 \quad \rho_3 = \sigma_1 S_p^2$$

B. CONTROLLER DESIGN

The efficiency of the system depends on the controller, which is designed in this paper. Therefore, the SMC algorithm needs to be optimized correctly to provide high performance.

Take (1) + (2):

$$m_s \ddot{z}_s + m_u \ddot{z}_u = K_T r - K_T z_u \tag{8}$$

Assuming that: $\frac{m_s \ddot{z}_s}{m_u \ddot{z}_u} \approx \kappa$

$$\Rightarrow \ddot{z}_s = \frac{K_T}{\kappa m_s} (r - z_u) \tag{9}$$

Let the state variables as follows:

$$\begin{matrix} x_1 = z_s & x_2 = \dot{z}_s & x_3 = z_u \\ x_4 = \dot{z}_u & x_5 = F_A \end{matrix}$$

Taking the derivative of state variables:

$$\begin{matrix} \dot{x}_1 = x_2 \\ \dot{x}_2 = \frac{1}{m_s} (-Kx_1 - Cx_2 + Kx_3 + Cx_4 + x_5) \\ \dot{x}_3 = x_4 \\ \dot{x}_4 = \frac{1}{m_u} (Kx_1 + Cx_2 - (K + K_T)x_3 - Cx_4 - x_5) \\ \dot{x}_5 = \rho_1 i(t) - \rho_3 x_2 + \rho_3 x_4 - \rho_2 x_5 \end{matrix}$$

Considering the output signal is the displacement of the sprung mass:

$$y = z_s = x_1 \tag{10}$$

Take the first derivative of the output signal:

$$\dot{y} = \dot{x}_1 = x_2 \tag{11}$$

Take the second derivative of the output signal:

$$\ddot{y} = \ddot{z}_s = \frac{K_T}{\kappa m_s} (r - x_3) \tag{12}$$

Derivative on both sides of equation (12), get:

$$\dddot{y} = \frac{K_T}{\kappa m_s} (\dot{r} - \dot{x}_3) \tag{13}$$

Similarly, considering the fourth and fifth-order derivatives of the output signal:

$$y^{(4)} = -\frac{K_T}{\kappa m_s m_u} \left(\begin{matrix} Kx_1 + Cx_2 - (K + K_T)x_3 \\ -Cx_4 - x_5 \end{matrix} \right) + \frac{K_T}{\kappa m_s} \ddot{r} \tag{14}$$

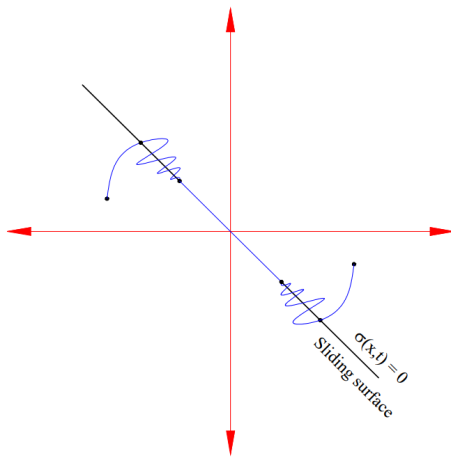


FIGURE 3. Sliding surface.

$$y^{(5)} = \frac{K_T}{\kappa m_s m_u} \begin{bmatrix} KC \left(\frac{1}{m_s} + \frac{1}{m_u} \right) x_1 \\ + \left(\frac{C^2}{m_s} + \frac{C^2}{m_u} - K - \rho_3 \right) x_2 \\ - C \left(\frac{K}{m_s} + \frac{K + K_T}{m_u} \right) x_3 \\ - \left(\frac{C^2}{m_s} + \frac{C^2}{m_u} - K - K_T - \rho_3 \right) x_4 \\ - \left(\frac{C}{m_s} + \frac{C}{m_u} + \rho_2 \right) x_5 \end{bmatrix} + \frac{K_T \rho_1}{\kappa m_s m_u} i(t) + \frac{K_T}{\kappa m_s} r \quad (15)$$

Assuming that $r(t)$ is the disturbance, so:

$$y^{(5)} \approx \vartheta_1 x_1 + \vartheta_2 x_2 + \vartheta_3 x_3 + \vartheta_4 x_4 + \vartheta_5 x_5 + \frac{K_T \rho_1}{\lambda m_s m_u} i(t) \quad (16)$$

where:

$$\begin{aligned} \vartheta_1 &= KC \left(\frac{1}{m_s} + \frac{1}{m_u} \right) \\ \vartheta_2 &= \left(\frac{C^2}{m_s} + \frac{C^2}{m_u} - K - \rho_3 \right) \\ \vartheta_3 &= -C \left(\frac{K}{m_s} + \frac{K + K_T}{m_u} \right) \\ \vartheta_4 &= - \left(\frac{C^2}{m_s} + \frac{C^2}{m_u} - K - K_T - \rho_3 \right) \\ \vartheta_5 &= - \left(\frac{C}{m_s} + \frac{C}{m_u} + \rho_2 \right) \end{aligned}$$

Let $e(t)$ be the error between the desired output signal y_s ($y_s \approx$ zero) and the actual output signal y

$$e(t) = y_s - y \quad (17)$$

To minimize the error, the object needs to be moved along the sliding surface (Figure 3). The sliding surface $\sigma(t)$ is a

function that depends on the error signal $e(t)$:

$$\sigma = \sum_{i=1}^n \sum_{j=0}^{n-1} \lambda_j e^{(n-i)} \quad (18)$$

Finally, the current control signal generated from the controller is defined as equation (19):

$$i(t) = \frac{\kappa m_s m_u}{K_T \rho_1} \begin{bmatrix} y_s^{(n)} - \sum_{k=1}^n \vartheta_k x_k + \sum_{i=1}^n \sum_{j=0}^{n-1} \lambda_j e^{(n-i)} \\ + T \text{sgn} \left(\sum_{m=0}^{n-1} \sum_{l=0}^{n-1} \lambda_m e^{(n-1-l)} \right) \end{bmatrix} \quad (19)$$

After the controller has been designed, the simulation is performed.

III. RESULTS

A. PARAMETERS OF THE SIMULATION PROCESS

The simulation is done in the MATLAB-Simulink environment. To make oscillation of the vehicle, excitations from the road surface are used. In this paper, four types of stimuli are proposed as shown in Figure 4. These types of stimuli correspond to the four investigated cases.

Case 1 and Case 2:

$$r(t) = A \sin(2\pi f t + \varphi) \quad (20)$$

Case 3 and Case 4:

$$\dot{r}(t) = 2\pi \left(\sqrt{Gv\omega(t)} - fr(t) \right) \quad (21)$$

where:

- v : Velocity
- G : Constant
- $\omega(t)$: White noise

In these cases, the amplitude and frequency of the oscillation are different.

The parameters of the reference vehicle are given in Table 1 [14].

With the input being stimuli from the pavement, the outputs include displacement of the sprung mass, acceleration of the sprung mass, displacement of the unsprung mass, and acceleration of the unsprung mass. These parameters are determined with the maximum value and the average value calculated according to the RMS.

$$f_{RMS} = \lim_{T \rightarrow \infty} \sqrt{\frac{1}{2T} \int_{-T}^T f^2(t) dt} \quad (22)$$

B. RESULTS AND DISCUSSIONS

Simulation is performed in the four cases mentioned above.

Case 1: In the first case, a sinusoidal pavement excitation is used. Accordingly, the displacement of the sprung mass changes with the stimulus from the pavement. This change is shown in Figure 5. In the first phase, the oscillation is not

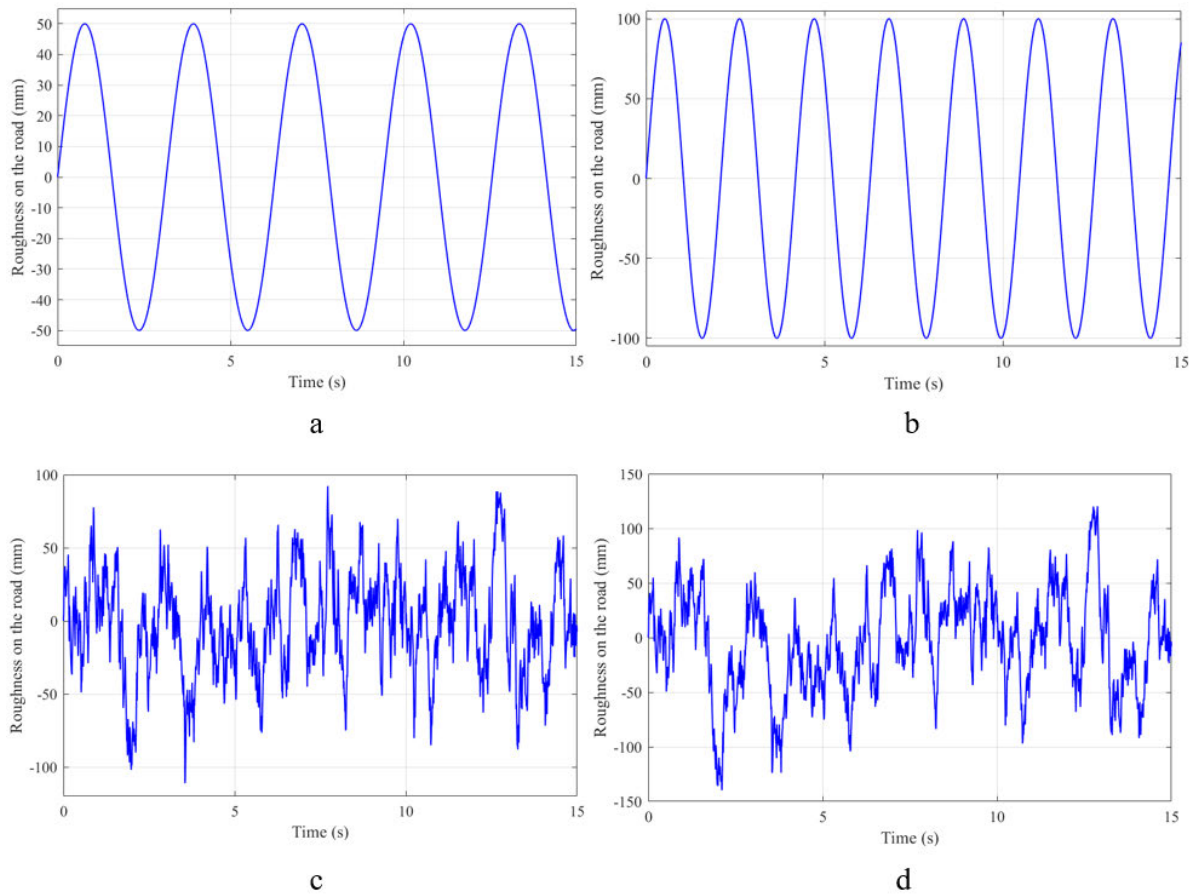


FIGURE 4. Roughness on the road (a-case 1, b-case 2, c-case 3, d-case 4).

TABLE 1. Parameters of the vehicle.

Description	Symbol	Value	Unit
Sprung mass	m_s	500	kg
Unsprung mass	m_u	55	kg
Spring coefficient	K	45×10^3	N/m
Tire coefficient	K_T	180×10^3	N/m
Damper coefficient	C	3.9×10^3	Ns/m
Actuator coefficient	ρ_1	4.5×10^{13}	N/m ⁵
Actuator coefficient	ρ_2	1	s ⁻¹
Actuator coefficient	ρ_3	1.5×10^9	N/kg ^{1/2} m ^{5/2}
Time constant	τ	2.5×10^{-3}	s
Piston cross-sectional area	S_p	3.5×10^{-4}	m ²
Supply pressure	P_s	1056350	N/m ²
Servo valve gain	k_{sv}	1×10^{-3}	m/V

stable. In the next phases, the amplitude of the oscillation is more stable and changes according to the cyclic law. The maximum values of displacement of the sprung mass are 52.9 (mm), 23.3 (mm), and 8.2 (mm) respectively for the three investigated situations. Besides, the average value calculated

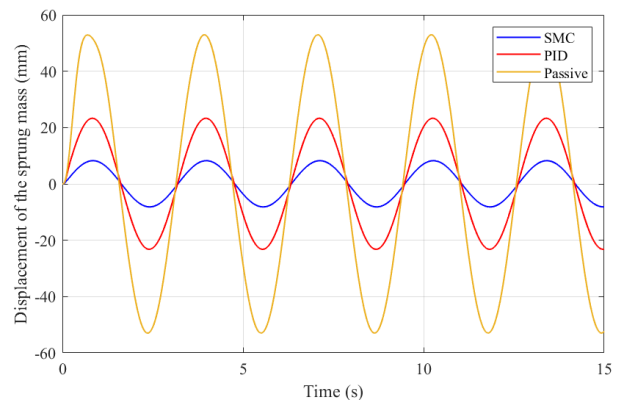


FIGURE 5. Displacement of the sprung mass (Case 1).

according to the RMS is 37.5 (mm), 16.4 (mm), and 5.8 (mm) respectively.

The acceleration of the sprung mass is used to assess the vehicle’s smoothness. Like above, in the initial phase, the acceleration is still unstable (Figure 6). This value changes cyclically starting from the second phase onwards. The maximum value of the acceleration of the sprung mass when the vehicle uses a passive suspension system is 0.87 (m/s²). If the active suspension system is used to

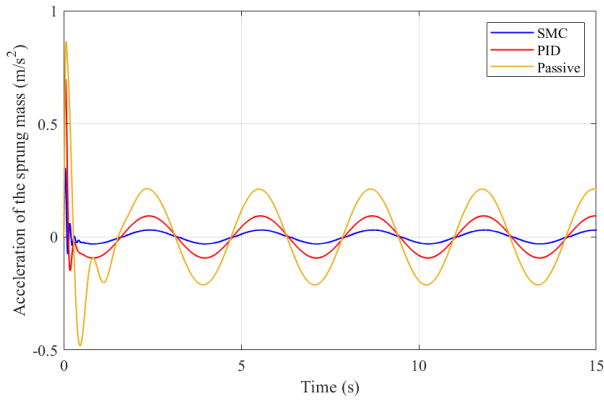


FIGURE 6. Acceleration of the sprung mass (Case 1).

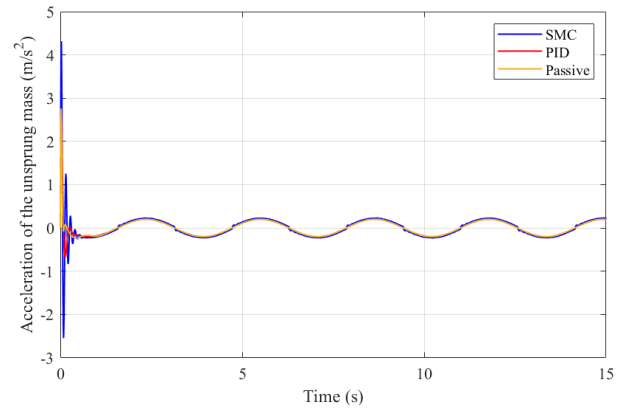


FIGURE 8. Acceleration of the unsprung mass (Case 1).

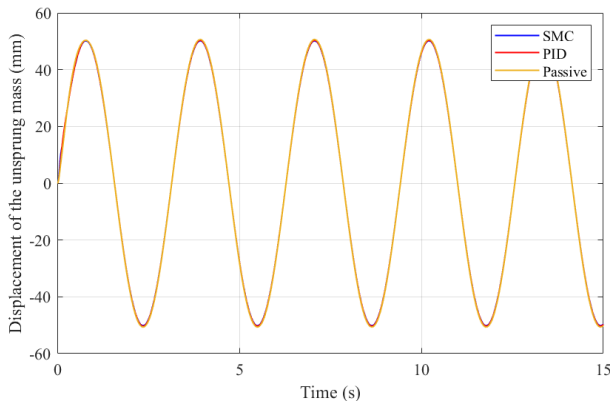


FIGURE 7. Displacement of the unsprung mass (Case 1).

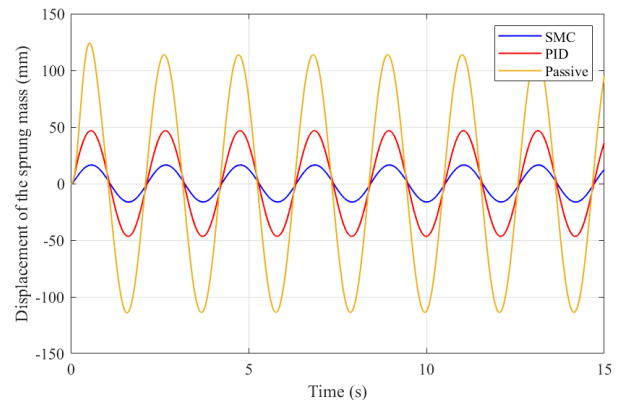


FIGURE 9. Displacement of the sprung mass (Case 2).

replace the conventional passive suspension system, the maximum value of the acceleration of the sprung mass will be reduced to only $0.70 \text{ (m/s}^2\text{)}$ and $0.31 \text{ (m/s}^2\text{)}$, respectively, for linear control and nonlinear control. In addition, the active suspension system also reduces the average value of acceleration significantly. According to (22), the average value of the acceleration of the sprung mass when the vehicle uses the SMC algorithm is only $0.03 \text{ (m/s}^2\text{)}$. Meanwhile, this value reaches $0.08 \text{ (m/s}^2\text{)}$ when the PID algorithm is used. In particular, this value can be up to $0.18 \text{ (m/s}^2\text{)}$ if the vehicle uses only passive suspension. The difference between the values can be up to 6 times.

The displacement of the unsprung mass does not greatly affect the vehicle’s oscillations. However, if this value is small, the smoothness of the vehicle will be improved more. According to the graph in Figure 7, the values of the displacement of the unsprung mass in all three situations are similar. The difference between them is not more than 1.5%. The value of the displacement of the unsprung mass following the input excitation signal.

The difference in acceleration of the unsprung mass is also small. At the initial instant, the acceleration of the unsprung mass reaches its maximum value. This value fluctuates steadily and closely follows each other in subsequent phases, their average values during the investigated period reached $0.19 \text{ (m/s}^2\text{)}$, $0.20 \text{ (m/s}^2\text{)}$, and $0.28 \text{ (m/s}^2\text{)}$, respectively.

Case 2: In the second case, the amplitude and frequency of the pavement excitation were increased. Therefore, the oscillation of the vehicle will also be larger. According to Figure 9, the maximum displacement of the sprung mass can be up to 124.1 (mm) if the vehicle uses only the mechanical suspension system. When the active suspension system with the PID algorithm is used, the maximum value of the oscillation reaches 46.7 (mm) . Besides, this value can decrease even more when the SMC algorithm is used, reaching 16.4 (mm) . The average value calculated according to RMS reached 80.0 (mm) , 32.8 (mm) , and 11.5 (mm) respectively for the situations.

Like the first case, in this case, the acceleration of the sprung mass is also unstable in the first phase (Figure 10). In subsequent phases, the acceleration of the sprung mass oscillates cyclically according to the excitation signal. The maximum acceleration is $2.58 \text{ (m/s}^2\text{)}$, $2.09 \text{ (m/s}^2\text{)}$, and $0.92 \text{ (m/s}^2\text{)}$, respectively. Besides, the average value of acceleration reached $0.78 \text{ (m/s}^2\text{)}$, $0.32 \text{ (m/s}^2\text{)}$, and $0.11 \text{ (m/s}^2\text{)}$. Obviously, the SMC algorithm helps to reduce the oscillation significantly.

The displacement of the unsprung mass (Figure 11) and the acceleration of the unsprung mass (Figure 12) tend to follow the excitation signal from the pavement. The difference between the values in the investigated situations is very small.

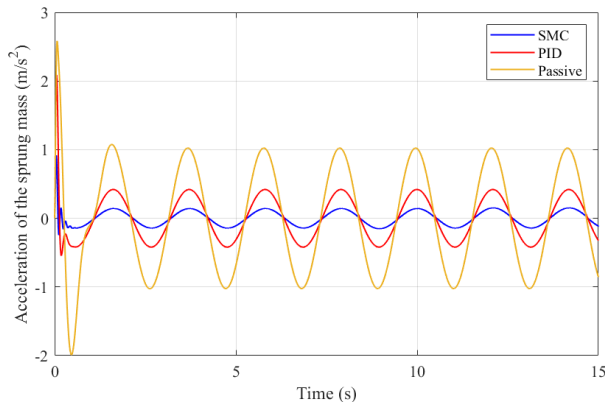


FIGURE 10. Acceleration of the sprung mass (Case 2).

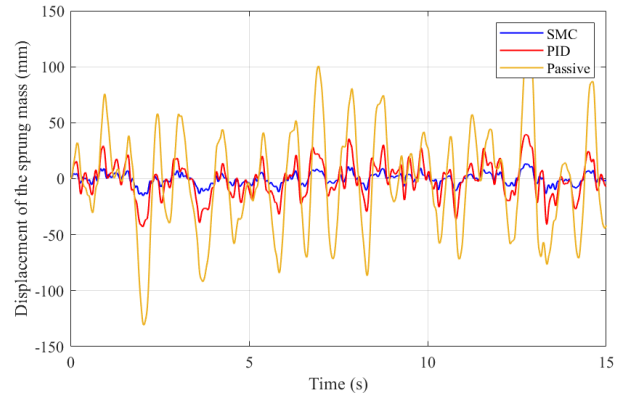


FIGURE 13. Displacement of the sprung mass (Case 3).

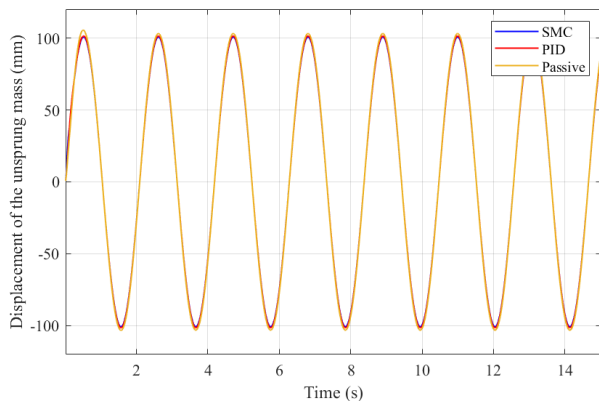


FIGURE 11. Displacement of the sprung mass (Case 2).

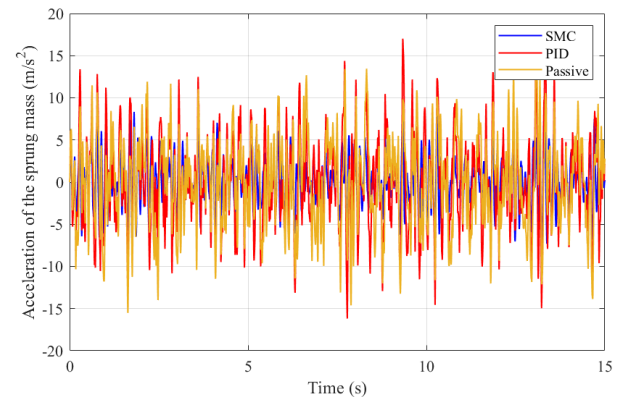


FIGURE 14. Acceleration of the sprung mass (Case 3).

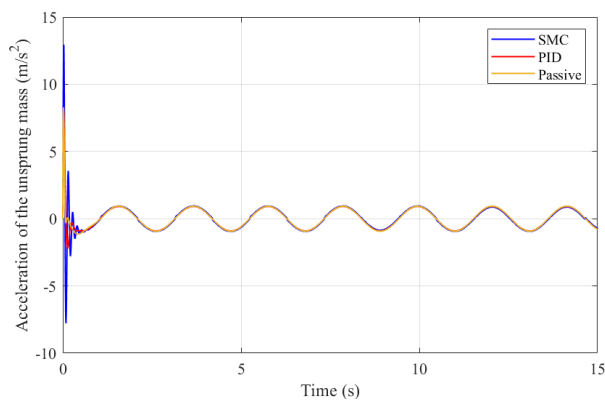


FIGURE 12. Acceleration of the unsprung mass (Case 2).

Case 3: In the third case, the vehicle’s oscillation has the standard random excitation form. The vehicle’s oscillations change continuously over time. This is shown in Figure 13. According to this result, the vehicle’s oscillation is very large when the vehicle only uses the conventional passive suspension system. The maximum value of displacement of the sprung mass is 133.1 (mm). This value is 8.8 times that of using the SMC algorithm for the active suspension system. The average value of the displacement of the sprung mass is also significantly reduced when the nonlinear control method is applied. It equals only 32.9% and 10.9% of the other two situations.

With random excitation, the acceleration of the sprung mass varies continuously with very large amplitude and frequency. The maximum values of acceleration are 18.20 (m/s²), 17.01 (m/s²), and 9.41 (m/s²), respectively. According to this result, the maximum value of acceleration when using the PID controller is approximately compared with the situation of the vehicle using the conventional passive suspension system. Therefore, the linear control algorithm cannot satisfy the conditions of stability and oscillation in this case. In contrast, the nonlinear controller with the SMC algorithm greatly reduces oscillation. Also, in this case, the average acceleration of the sprung mass when using the PID controller is greater than that of the vehicle using the passive suspension system. These values are 5.30 (m/s²) and 5.25 (m/s²), respectively. Meanwhile, the value calculated according to the RMS of the SMC algorithm is only 3.05 (m/s²), only about 58% compared to the two situations mentioned above.

For an active suspension system, to reduce the oscillations of the sprung mass, the hydraulic actuator needs to operate continuously. Therefore, the oscillations of the unsprung mass will be affected (Figure 15 and Figure 16). In fact, the values for the displacement and acceleration of the unsprung mass when using an active suspension will be larger than that of a conventional passive suspension system.

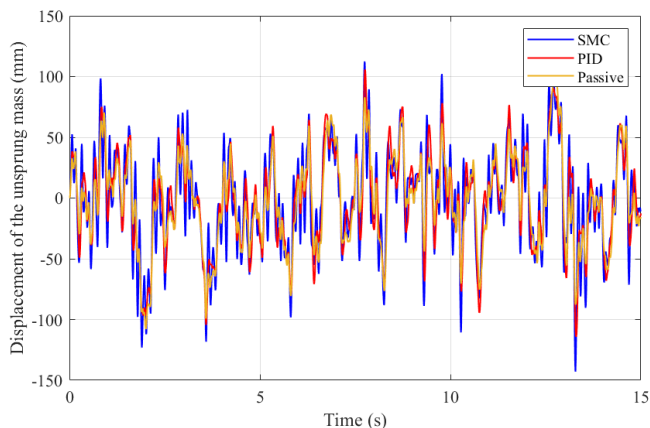


FIGURE 15. Displacement of the unsprung mass (Case 3).

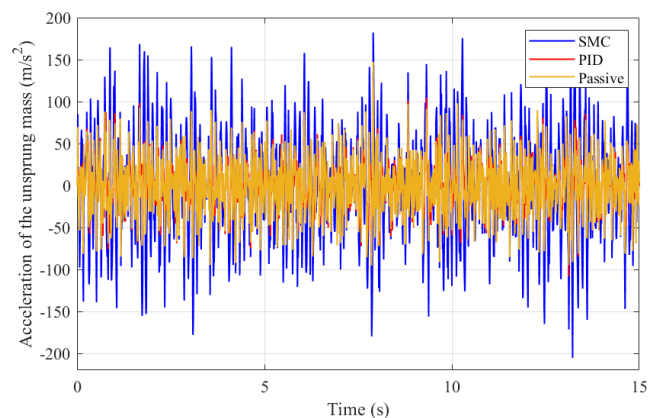


FIGURE 16. Acceleration of the unsprung mass (Case 3).

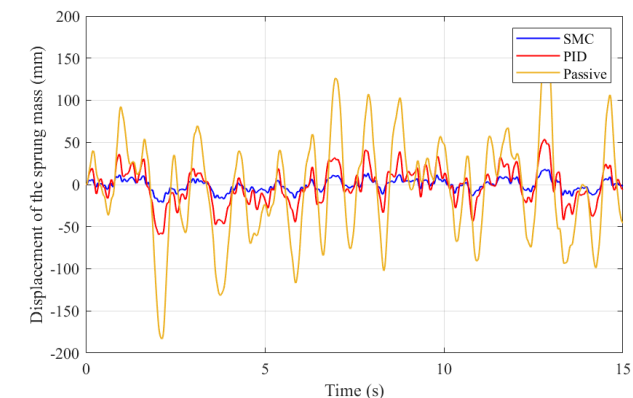


FIGURE 17. Displacement of the sprung mass (Case 4).

This is completely reasonable. It does not affect the overall oscillation of the vehicle.

Case 4: In this case, the pavement excitation takes on a random form with a larger amplitude than in the third case. As the excitation amplitude increases, the vehicle’s oscillation will also become stronger. The average value of the displacement of the sprung mass reached 62.3 (mm), 21.4 (mm), and 7.2 (mm) respectively for the three investigated situations. Meanwhile, if the vehicle uses a passive suspension system, the maximum value of displacement can be 8.6 times that of

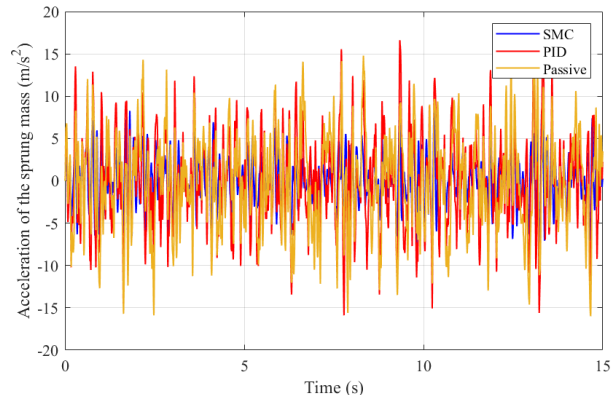


FIGURE 18. Acceleration of the sprung mass (Case 4).

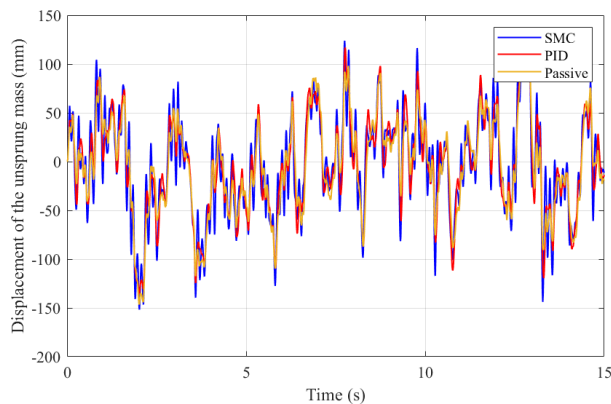


FIGURE 19. Displacement of the unsprung mass (Case 4).

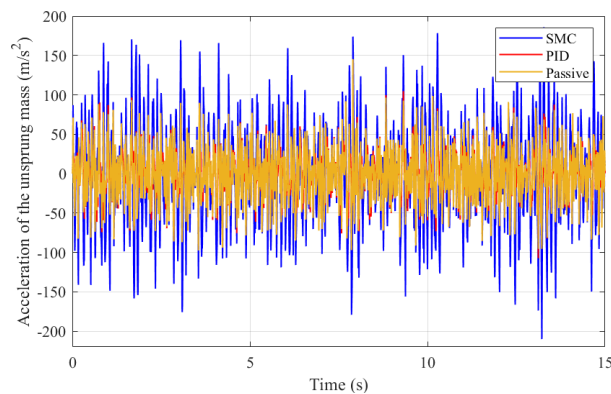


FIGURE 20. Acceleration of the unsprung mass (Case 4).

an active suspension system controlled by the SMC algorithm (Figure 17).

The SMC algorithm helps control the vehicle’s oscillation more effectively than the PID algorithm. Based on the graph of Figure 18, the maximum and average values of acceleration when using the PID controller are even larger than using the passive suspension system. These values are 5.40 (m/s²) and 5.57 (m/s²), 17.43 (m/s²) and 17.13 (m/s²), respectively. Meanwhile, the value of the nonlinear controller is only 3.08 (m/s²) and 9.44 (m/s²). This value is much lower than the two situations mentioned above.

TABLE 2. The maximum value of the sprung mass.

	<i>Displacement of the sprung mass (mm)</i>			<i>Acceleration of the sprung mass (m/s²)</i>		
	<i>Passive</i>	<i>PID</i>	<i>SMC</i>	<i>Passive</i>	<i>PID</i>	<i>SMC</i>
Case 1	52.9	23.3	8.2	0.87	0.70	0.31
Case 2	124.1	46.7	16.4	2.58	2.09	0.92
Case 3	133.1	43.1	15.2	18.20	17.01	9.41
Case 4	183.1	59.2	21.3	17.13	17.43	9.44

TABLE 3. The average value of the sprung mass.

	<i>Displacement of the sprung mass (mm)</i>			<i>Acceleration of the sprung mass (m/s²)</i>		
	<i>Passive</i>	<i>PID</i>	<i>SMC</i>	<i>Passive</i>	<i>PID</i>	<i>SMC</i>
Case 1	37.5	16.4	5.8	0.18	0.08	0.03
Case 2	80.0	32.8	11.5	0.78	0.32	0.11
Case 3	47.4	15.8	5.2	5.25	5.30	3.05
Case 4	62.3	21.4	7.2	5.57	5.40	3.08

TABLE 4. Percent of maximum value.

	<i>Displacement of the sprung mass (%)</i>			<i>Acceleration of the sprung mass (%)</i>		
	<i>Passive</i>	<i>PID</i>	<i>SMC</i>	<i>Passive</i>	<i>PID</i>	<i>SMC</i>
Case 1	100.0	44.0	15.5	100.0	80.5	35.6
Case 2	100.0	37.6	13.2	100.0	81.0	35.7
Case 3	100.0	32.4	11.4	100.0	93.5	51.7
Case 4	100.0	32.3	11.6	100.0	101.8	55.1

As the excitation from the pavement increases, the displacement and acceleration of the unsprung mass also increase accordingly. There is a relative difference in the values of the displacement and acceleration of the unsprung mass in the simulated situations. However, the smoothness of the vehicle is still guaranteed to be stable.

The results of the simulation process are summarized in Table 2 and Table 3. The ratios between these values are shown in Table 4 and Table 5.

There are two main conflicting parameters which are riding comfort and handling stability. In this research, the quarter dynamics vehicle is used. Therefore, the ride comfort of the

TABLE 5. Percent of average value.

	Displacement of the sprung mass (%)			Acceleration of the sprung mass (%)		
	Passive	PID	SMC	Passive	PID	SMC
Case 1	100.0	43.7	15.5	100.0	44.4	16.7
Case 2	100.0	41.0	14.4	100.0	41.0	14.1
Case 3	100.0	33.3	11.0	100.0	101.0	58.1
Case 4	100.0	34.3	11.6	100.0	96.9	55.3

vehicle is only considered. Problems of handling stability will be considered in other studies.

IV. CONCLUSION

This research is aimed at improving a vehicle's oscillation based on an active suspension system. In this paper, a quarter dynamics model is used to simulate the vehicle's oscillations. Besides, the dynamics model of the hydraulic actuator is also linearized accordingly. To ensure the stable performance of the controller in different moving cases, the SMC algorithm is proposed to be used. This is a nonlinear control method that helps the output signal follow the set signal.

The cause of the oscillation is the excitation from the pavement. Therefore, the author has introduced four stimulus cases corresponding to the actual moving conditions of the vehicle. Based on the reference parameters, the calculation and simulation are carried out in the MATLAB-Simulink environment. The simulation process includes three situations: a vehicle using a passive suspension, a vehicle using an active suspension controlled by the PID algorithm, and a vehicle using an active suspension controlled by the SMC algorithm.

The results of the research showed the superiority of the SMC algorithm used in this paper. Accordingly, the displacement and acceleration of the sprung mass were significantly reduced when the nonlinear control algorithm was used. The maximum value and average value of oscillations are guaranteed within the allowable limits. In the investigated cases, the system always ensures stability and sustainability. Therefore, the smoothness and comfort of the vehicle have been enhanced.

The SMC control algorithm brings positivity to complex oscillating systems. However, this is a nonlinear control method. Therefore, the design and optimization process are quite complex. In some cases, the "chattering" phenomenon can still occur. To improve system efficiency, some intelligent control algorithms should be combined with SMC algorithms

such as Fuzzy SMC, Neural SMC, etc. In the future, experiments on the nonlinear control algorithm for the suspension system need to be conducted to demonstrate the effectiveness of the research.

NOMENCLATURE

F_A	: Force of the actuator, N.
F_C	: Force of the damper, N.
F_K	: Force of the spring, N.
F_{KT}	: Force of the tire, N.
r	: Roughness on the road, m.
z_s	: Displacement of the sprung mass, m.
z_u	: Displacement of the unsprung mass, m.

ABBREVIATION

ANN	: Artificial Neural Network.
LPV	: Linear Parameters Varying.
LQG	: Linear Quadratic Gaussian.
LQR	: Linear Quadratic Regulator.
MIMO	: Multi-Input Multi-Output.
PID	: Proportional Integral Derivative.
RMS	: Root Mean Square.
SISO	: Single-Input Single-Output.
SMC	: Sliding Mode Control.

REFERENCES

- [1] I. Mihai and F. Andronic, "Behavior of a semi-active suspension system versus a passive suspension system on an uneven road surface," *Mechanics*, vol. 20, no. 1, pp. 64–69, Mar. 2014, doi: [10.5755/j01.mech.20.1.6591](https://doi.org/10.5755/j01.mech.20.1.6591).
- [2] S. A. Patil and S. G. Joshi, "Experimental analysis of 2 DOF quarter-car passive and hydraulic active suspension systems for ride comfort," *Syst. Sci. Control Eng.*, vol. 2, no. 1, pp. 621–631, Dec. 2014, doi: [10.1080/21642583.2014.913212](https://doi.org/10.1080/21642583.2014.913212).
- [3] K. Hudha and H. Jamaluddin, "Simulation and experimental evaluation on a skyhook policy-based fuzzy logic control for semi-active suspension system," *Int. J. Struct. Eng.*, vol. 2, no. 3, pp. 243–272, 2011, doi: [10.1504/IJSTRUCTE.2011.040783](https://doi.org/10.1504/IJSTRUCTE.2011.040783).
- [4] P. K. Eskandary, A. Khajepour, A. Wong, and M. Ansari, "Analysis and optimization of air suspension system with independent height and stiffness tuning," *Int. J. Automot. Technol.*, vol. 17, no. 5, pp. 807–816, Oct. 2016, doi: [10.1007/s12239-016-0079-9](https://doi.org/10.1007/s12239-016-0079-9).

- [5] T. A. Nguyen, "Advance the stability of the vehicle by using the pneumatic suspension system integrated with the hydraulic actuator," *Latin Amer. J. Solids Struct.*, vol. 18, no. 7, 2021, Art. no. e403, doi: [10.1590/1679-78256621](https://doi.org/10.1590/1679-78256621).
- [6] H. Basargan, A. Mihály, P. Gáspár, and O. Sename, "Adaptive semi-active suspension and cruise control through LPV technique," *Appl. Sci.*, vol. 11, no. 1, p. 290, Dec. 2020, doi: [10.3390/app11010290](https://doi.org/10.3390/app11010290).
- [7] Y. M. Khedkar, S. Bhat, and H. Adarsha, "A review of magnetorheological fluid damper technology and its applications," *Int. Rev. Mech. Eng.*, vol. 13, no. 4, pp. 256–264, 2019, doi: [10.15866/ireme.v13i4.17224](https://doi.org/10.15866/ireme.v13i4.17224).
- [8] I. T. Jiregna and G. Sirata, "A review of the vehicle suspension system," *J. Mech. Energy Eng.*, vol. 4, no. 2, pp. 109–114, Nov. 2020, doi: [10.30464/jmee.2020.4.2.109](https://doi.org/10.30464/jmee.2020.4.2.109).
- [9] Q. Zhao and B. Zhu, "Multi-objective optimization of active suspension predictive control based on improved PSO algorithm," *J. Vibroeng.*, vol. 21, no. 5, pp. 1388–1404, Aug. 2019, doi: [10.21595/jve.2018.19580](https://doi.org/10.21595/jve.2018.19580).
- [10] N. T. Anh, "Control an active suspension system by using PID and LQR controller," *Int. J. Mech. Prod. Eng. Res. Develop.*, vol. 10, no. 3, pp. 7003–7012, 2020, doi: [10.24247/ijmperdjun2020662](https://doi.org/10.24247/ijmperdjun2020662).
- [11] M. Haddar, R. Chaari, S. C. Baslamisli, F. Chaari, and M. Haddar, "Intelligent PD controller design for active suspension system based on robust model-free control strategy," *Proc. Inst. Mech. Eng., C, J. Mech. Eng. Sci.*, vol. 233, no. 14, pp. 4863–4880, Jul. 2019, doi: [10.1177/0954406219836443](https://doi.org/10.1177/0954406219836443).
- [12] H. Metered, W. Abbas, and A. S. Emam, "Optimized proportional integral derivative controller of vehicle active suspension system using genetic algorithm," SAE Tech. Paper 2018-01-1399, 2018, doi: [10.4271/2018-01-1399](https://doi.org/10.4271/2018-01-1399).
- [13] M. Heidari and H. Homaei, "Design a PID controller for suspension system by back propagation neural network," *J. Eng.*, vol. 2013, pp. 1–9, Feb. 2013, doi: [10.1155/2013/421543](https://doi.org/10.1155/2013/421543).
- [14] T. A. Nguyen, "Improving the comfort of the vehicle based on using the active suspension system controlled by the double-integrated controller," *Shock Vib.*, vol. 2021, pp. 1–11, Sep. 2021, doi: [10.1155/2021/1426003](https://doi.org/10.1155/2021/1426003).
- [15] M. P. Nagarkar, G. J. Vikhe, K. R. Borole, and V. M. Nandedkar, "Active control of quarter car suspension system using linear quadratic regulator," *Int. J. Automot. Mech. Eng.*, vol. 3, pp. 364–372, Jun. 2011, doi: [10.15282/ijame.3.2011.11.0030](https://doi.org/10.15282/ijame.3.2011.11.0030).
- [16] L. Chai and T. Sun, "The design of LQG controller for active suspension based on analytic hierarchy process," *Math. Problems Eng.*, vol. 2010, pp. 1–19, Jul. 2010, doi: [10.1155/2010/701951](https://doi.org/10.1155/2010/701951).
- [17] R.-X. Xia, J.-H. Li, J. He, D.-F. Shi, and Y. Zhang, "Linear-quadratic-Gaussian controller for truck active suspension based on cargo integrity," *Adv. Mech. Eng.*, vol. 7, no. 12, pp. 1–9, Dec. 2015, doi: [10.1177/1687814015620320](https://doi.org/10.1177/1687814015620320).
- [18] H. Pang, Y. Chen, J. Chen, and X. Liu, "Design of LQG controller for active suspension without considering road input signals," *Shock Vib.*, vol. 2017, pp. 1–13, Feb. 2017, doi: [10.1155/2017/6573567](https://doi.org/10.1155/2017/6573567).
- [19] O. Gomonwattanapanich, N. Pannucharoenwong, P. Rattanadecho, S. Echaroj, and S. Hemathulin, "Vibration control of vehicle by active suspension with LQG algorithm," *Int. J. Automot. Mech. Eng.*, vol. 17, no. 2, pp. 8011–8018, 2020, doi: [10.15282/ijame.17.2.2020.19.0600](https://doi.org/10.15282/ijame.17.2.2020.19.0600).
- [20] S.-A. Chen, Y.-M. Cai, J. Wang, and M. Yao, "A novel LQG controller of active suspension system for vehicle roll safety," *Int. J. Control, Autom. Syst.*, vol. 16, no. 5, pp. 2203–2213, Oct. 2018, doi: [10.1007/s12555-017-0159-2](https://doi.org/10.1007/s12555-017-0159-2).
- [21] D. Rodriguez-Guevara, A. Favela-Contreras, F. Beltran-Carbajal, D. Sotelo, and C. Sotelo, "Active suspension control using an MPC-LQR-LPV controller with attraction sets and quadratic stability conditions," *Mathematics*, vol. 9, no. 20, p. 2533, Oct. 2021, doi: [10.3390/math9202533](https://doi.org/10.3390/math9202533).
- [22] F. Zhao, S. S. Ge, F. Tu, Y. Qin, and M. Dong, "Adaptive neural network control for active suspension system with actuator saturation," *IET Control Theory Appl.*, vol. 10, no. 14, pp. 1696–1705, Sep. 2016, doi: [10.1049/iet-cta.2015.1317](https://doi.org/10.1049/iet-cta.2015.1317).
- [23] Y. Huang, J. Na, X. Wu, G.-B. Gao, and Y. Guo, "Robust adaptive control for vehicle active suspension systems with uncertain dynamics," *Trans. Inst. Meas. Control*, vol. 40, no. 4, pp. 1237–1249, 2016, doi: [10.1177/0142331216678312](https://doi.org/10.1177/0142331216678312).
- [24] Z.-J. Fu, B. Li, X.-B. Ning, and W.-D. Xie, "Online adaptive optimal control of vehicle active suspension systems using single-network approximate dynamic programming," *Math. Problems Eng.*, vol. 2017, pp. 1–9, Apr. 2017, doi: [10.1155/2017/4575926](https://doi.org/10.1155/2017/4575926).
- [25] F. Zhao, M. Dong, Y. Qin, L. Gu, and J. Guan, "Adaptive neural networks control for camera stabilization with active suspension system," *Adv. Mech. Eng.*, vol. 7, no. 8, pp. 1–11, Aug. 2015, doi: [10.1177/1687814015599926](https://doi.org/10.1177/1687814015599926).
- [26] M. Faraji-Niri and F. Khani, "Robust guaranteed-cost control for half-vehicle active suspension systems subject to Markovian controller uncertainties," *IETE J. Res.*, pp. 1–9, Mar. 2021, doi: [10.1080/03772063.2021.1905083](https://doi.org/10.1080/03772063.2021.1905083).
- [27] C. Wang, K. Deng, W. Zhao, G. Zhou, and X. Li, "Robust control for active suspension system under steering condition," *Sci. China Technol. Sci.*, vol. 60, no. 2, pp. 199–208, Feb. 2017, doi: [10.1007/s11431-016-0423-9](https://doi.org/10.1007/s11431-016-0423-9).
- [28] C. Y. Yuan, Y. F. Teng, and X. Y. Yin, "Study of active suspension based on fuzzy neural network control," *Appl. Mech. Mater.*, vol. 251, pp. 201–205, Dec. 2012, doi: [10.4028/www.scientific.net/AMM.251.201](https://doi.org/10.4028/www.scientific.net/AMM.251.201).
- [29] M. Soleymani, M. Montazeri-Gh, and R. Amiryan, "Adaptive fuzzy controller for vehicle active suspension system based on traffic conditions," *Scientia Iranica*, vol. 19, no. 3, pp. 443–453, Jun. 2012, doi: [10.1016/j.scient.2012.03.002](https://doi.org/10.1016/j.scient.2012.03.002).
- [30] J. Na, Y. Huang, X. Wu, S. Su, and G. Li, "Adaptive finite-time fuzzy control of nonlinear active suspension systems with input delay," *IEEE Trans. Cybern.*, vol. 50, no. 6, pp. 2639–2650, Jun. 2020, doi: [10.1109/TCYB.2019.2894724](https://doi.org/10.1109/TCYB.2019.2894724).
- [31] J. Mrazgva, R. Chaibi, E. H. Tissir, and M. Ouahi, "Static output feedback stabilization of T-S fuzzy active suspension systems," *J. Terramech.*, vol. 97, pp. 19–27, Oct. 2021, doi: [10.1016/j.jterra.2021.05.001](https://doi.org/10.1016/j.jterra.2021.05.001).
- [32] B. Lin, X. Su, and X. Li, "Fuzzy sliding mode control for active suspension system with proportional differential sliding mode observer," *Asian J. Control*, vol. 21, no. 1, pp. 1–13, 2019, doi: [10.1002/asjc.1882](https://doi.org/10.1002/asjc.1882).
- [33] J. Zhang, K. Li, and Y. Li, "Neuro-adaptive optimized control for full active suspension systems with full state constraints," *Neurocomputing*, vol. 458, pp. 478–489, Oct. 2021, doi: [10.1016/j.neucom.2021.06.069](https://doi.org/10.1016/j.neucom.2021.06.069).
- [34] A. M. Al Aela, J.-P. Kenne, and H. A. Mintsa, "Adaptive neural network and nonlinear electrohydraulic active suspension control system," *J. Vib. Control*, pp. 1–17, Nov. 2020, doi: [10.1177/1077546320975979](https://doi.org/10.1177/1077546320975979).
- [35] T. A. Nguyen, "Study on the sliding mode control method for the active suspension system," *Int. J. Appl. Sci. Eng.*, vol. 18, no. 5, 2021, Art. no. 2021069, doi: [10.6703/IJASE.202109_18\(5\).006](https://doi.org/10.6703/IJASE.202109_18(5).006).
- [36] R. Bai and D. Guo, "Sliding-mode control of the active suspension system with the dynamics of a hydraulic actuator," *Complexity*, vol. 2018, pp. 1–6, Aug. 2018, doi: [10.1155/2018/5907208](https://doi.org/10.1155/2018/5907208).
- [37] J. Sun and K. Zhao, "Adaptive neural network sliding mode control for active suspension systems with electrohydraulic actuator dynamics," *Int. J. Adv. Robot. Syst.*, vol. 17, no. 4, pp. 1–11, Jul. 2020, doi: [10.1177/1729881420941986](https://doi.org/10.1177/1729881420941986).
- [38] U. N. L. T. Alves, J. P. F. Garcia, M. C. M. Teixeira, S. C. Garcia, and F. B. Rodrigues, "Sliding mode control for active suspension system with data acquisition delay," *Math. Problems Eng.*, vol. 2014, pp. 1–13, 2014, doi: [10.1155/2014/529293](https://doi.org/10.1155/2014/529293).
- [39] S. Wei and X. Su, "Sliding mode control design for active suspension systems using quantum particle swarm optimisation," *Int. J. Veh. Des.*, vol. 81, nos. 1–2, pp. 93–114, 2019.
- [40] M. M. Zirkohi and T.-C. Lin, "Interval type-2 fuzzy-neural network indirect adaptive sliding mode control for an active suspension system," *Nonlinear Dyn.*, vol. 79, no. 1, pp. 513–526, Jan. 2015, doi: [10.1007/s11071-014-1683-8](https://doi.org/10.1007/s11071-014-1683-8).



TUAN ANH NGUYEN was born in Hanoi, Vietnam, in 1995. He received the Engineering and master's degrees from the Hanoi University of Science and Technology (HUST), in 2018 and 2019, respectively. He is currently pursuing the Ph.D. degree. His majors are automotive engineering, vehicle dynamics, and optimization and control.

He is also a Lecturer with the Department of Automotive Engineering, Thuyloi University (TLU). He has more than 15 papers that have been published.

• • •